Broad-band Spectroscopy of X-ray Binary Pulsars

Sachindra Naik
Physical Research Laboratory, India

Accretion powered Binary X-Ray Pulsars

- *Flux of matter falling from stellar wind (HMXBs) or Roche lobe overflow (LMXBs)*
- *Interaction with the magnetic field at the magnetospheric radius*
- *Threading of magnetic field lines*
- *Formation of accreting columns or slabs of matter at the polar caps :*

  Source of X-ray radiation

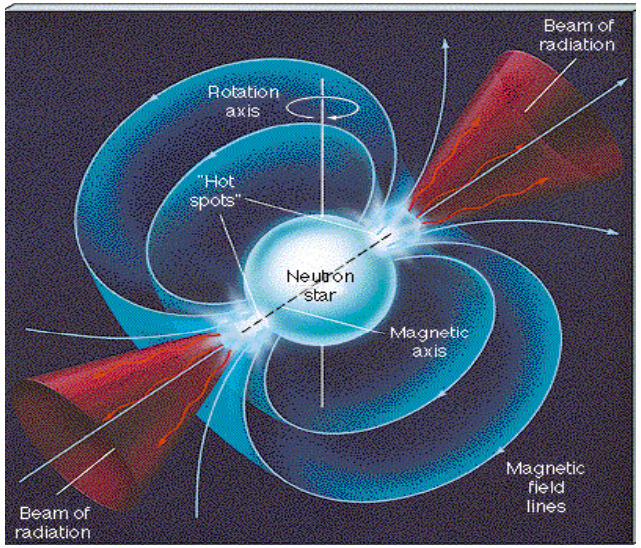

Broad-band Spectra in XRBPs

can be characterized by following components

- *Continuum Spectrum*
- *Line of sight absorption*
- *Soft excess*
- *Break/cutoff energy*
- *Emission line features*
- *Cyclotron resonance features*
- *Orbital phase dependent*
- *Pulse phase dependent*

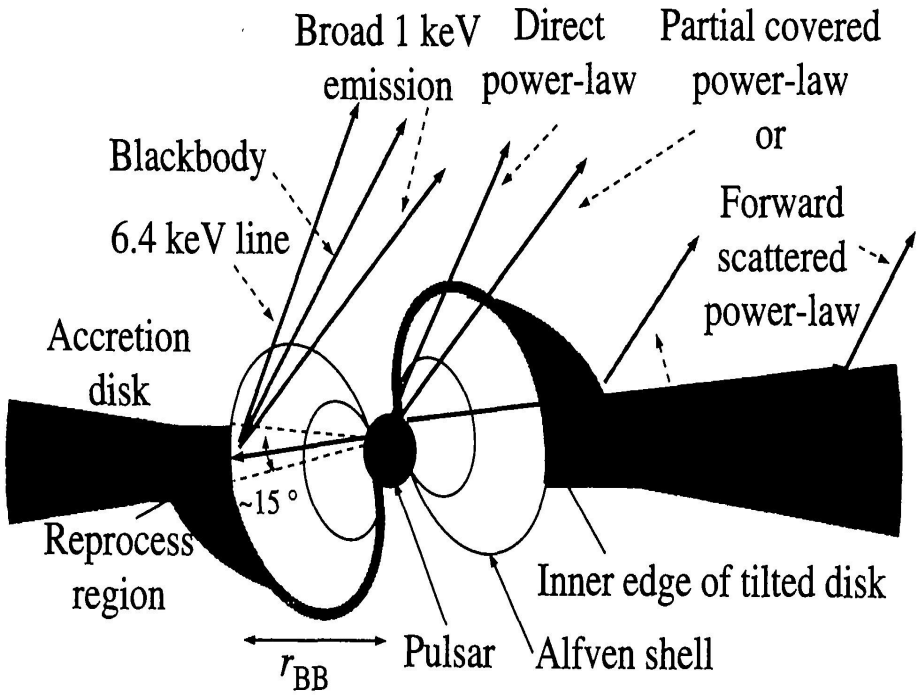

Endo et al. 2000

Broad-band Spectra in XRBPs

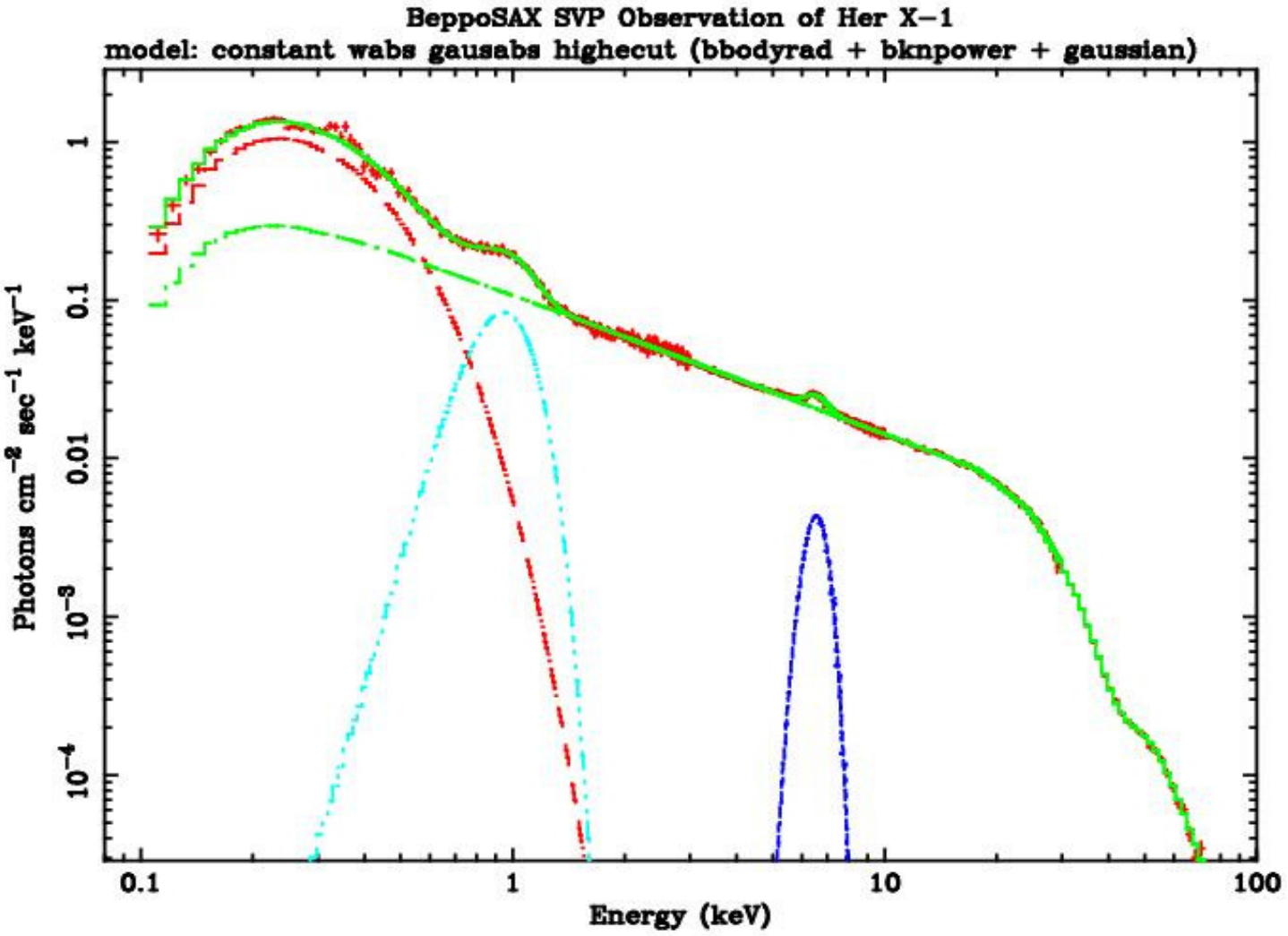

Broad-band Continuum in XRBPs

Continuum Spectrum:

1 : Power law modified by a high energy cutoff:

This was the very first empirical spectral model used to describe the XRBP continuum reasonably well (White et al. 1983).

$$\mathrm{POHI}(E) = \begin{cases} E^{-\alpha} & E < E_{\mathrm{cut}} \\ E^{-\alpha} \exp\left(-\dfrac{E - E_{\mathrm{cut}}}{E_{\mathrm{f}}}\right) & E > E_{\mathrm{cut}} \end{cases}$$

$$\mathrm{FDCO}(E) = \frac{1}{1 + \exp\left(\dfrac{E - E_{\mathrm{cut}}}{E_{\mathrm{f}}}\right)}$$

Tanaka 1986

Broad-band Continuum Model in XRBPs

2 : NPEX (Negative and Positive power law with EXponential cut-off): Makishima & Mihara (1995) introduced a more physical model to describe well Ginga XRBP spectra in 3–30 keV. At low energies, this model reduces to a simple power law with negative slope that is used to describe the XRBP spectra.

$$NPEX(E) = (AE^{-\alpha 1} + BE^{+\alpha 2}) \; exp\,(-E/kT)$$

This is an approximation of the unsaturated thermal Comptonization in hot plasma (Makishima et al. 1999).

3 : Partial covering high energy cut-off power law model :
This model consists of two power-law continua with a common photon index but with different hydrogen-absorbing column densities.

$$N(E) = e^{-\sigma(E)NH1} \; (S1 + S2 \; e^{-\sigma(E)NH2}) \; E^{-\Gamma} \; I(E)$$

where $I(E) = 1 \quad for \; E < E_c$

$= e^{-(E - E_c / E_f)} \quad for \; E > E_c$

Soft Excess in XRBPs

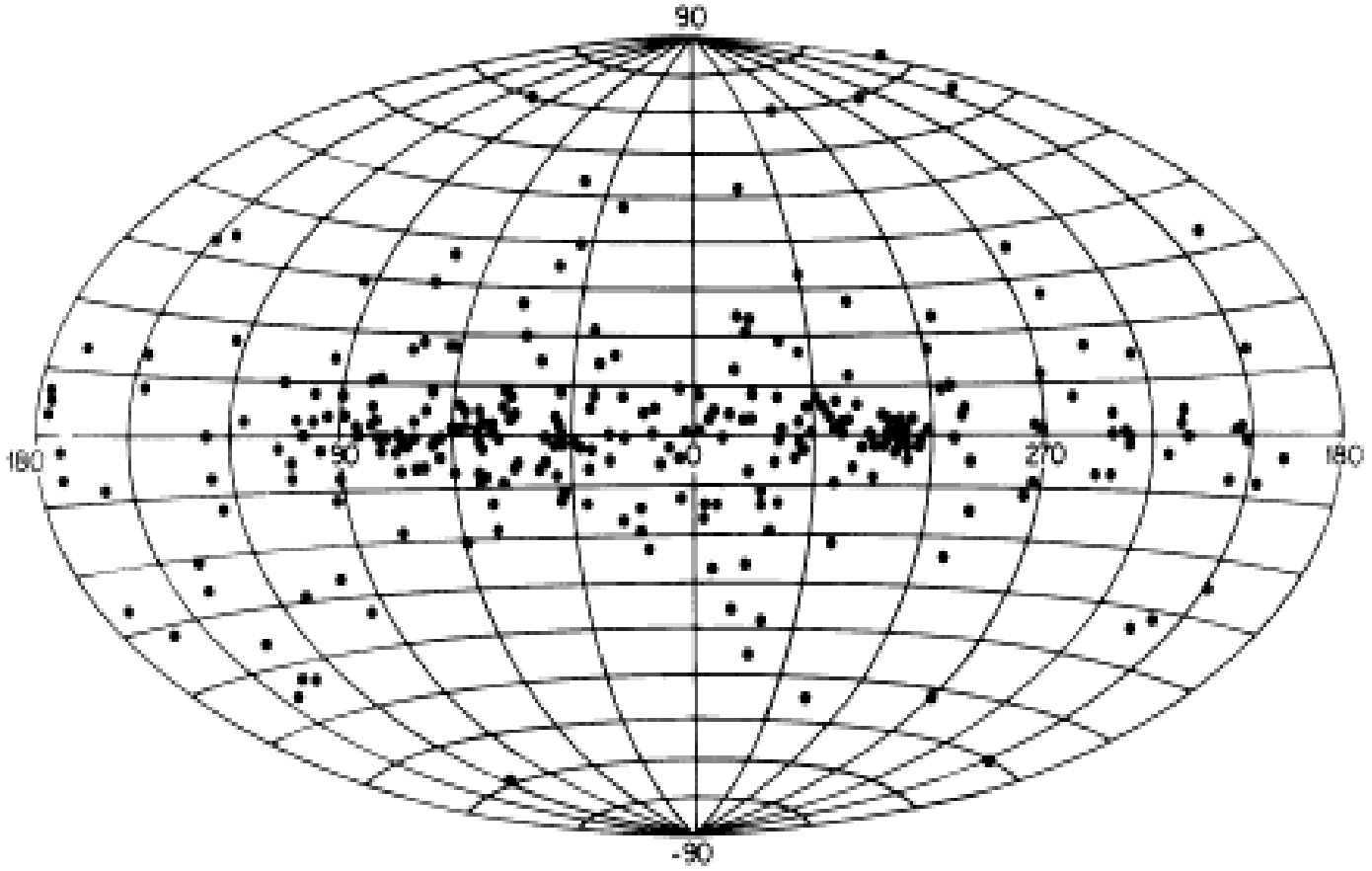

- **Soft excess is a common feature of emission from X-ray binary pulsars**
- **Observations that have not shown a soft excess are most often limited by low flux, high absorbing column, or insufficient sensitivity.**

Soft Excess in XRBPs

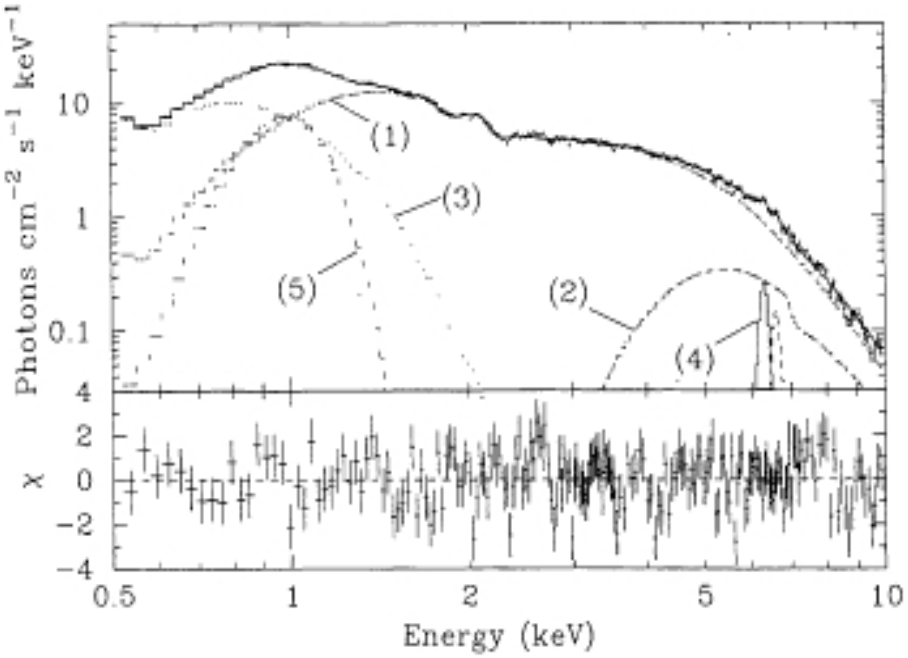

Her X-1, PP = 1.24 s,

- Blackbody
- Pulsating??

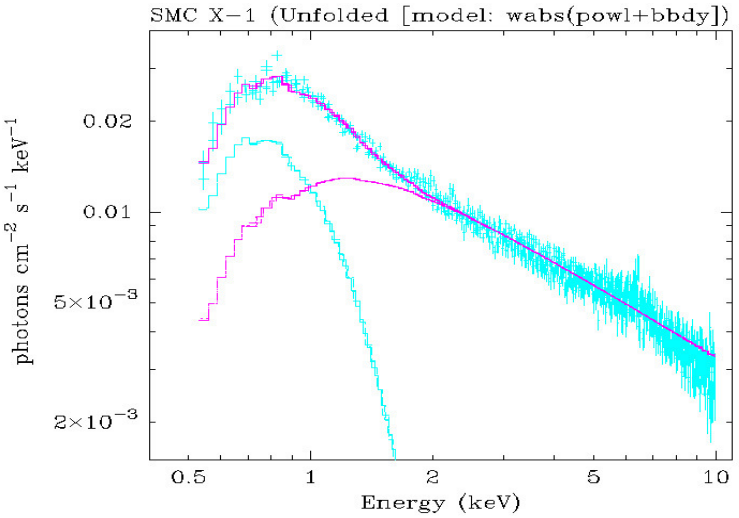

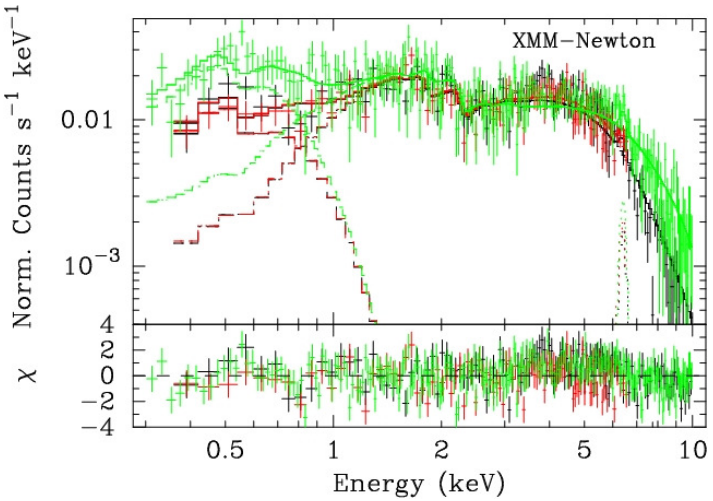

EXO 053109-6609.2, PP = 13.7 s,

Pulsation in soft component

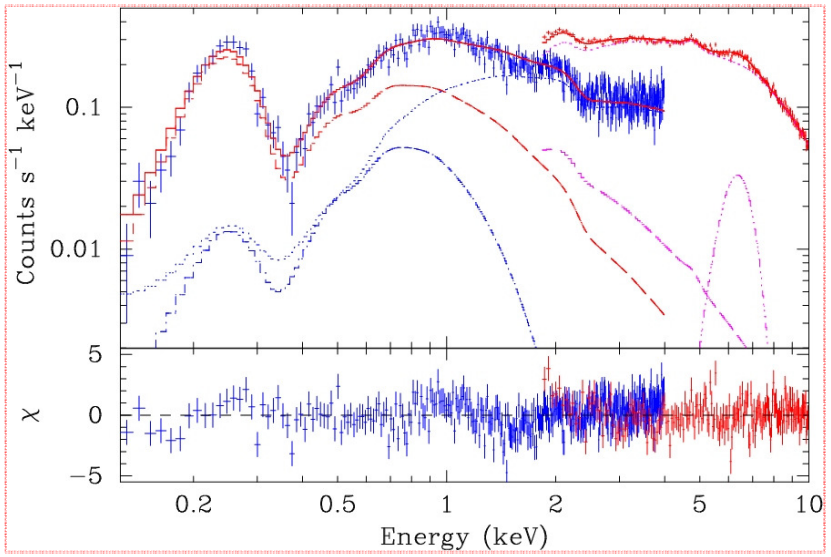

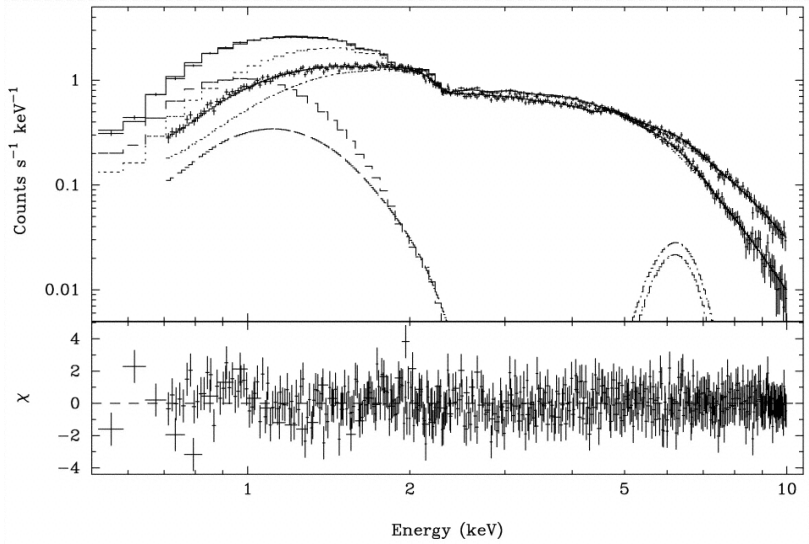

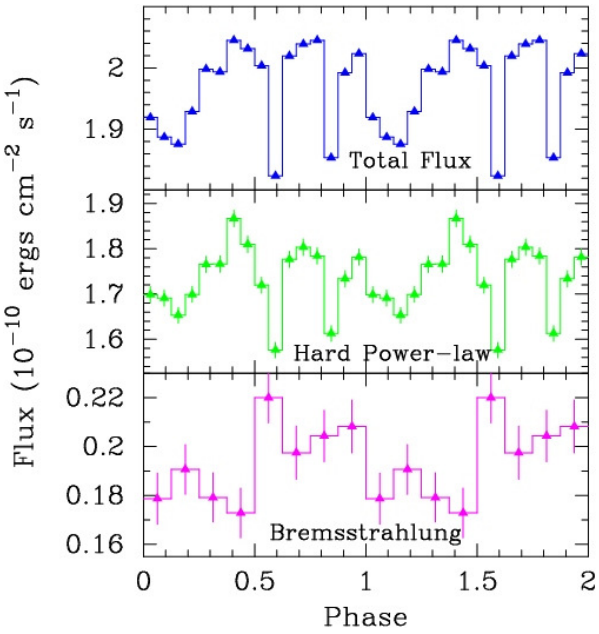

LMC X-4: PP = 13.5 s

(Naik & Paul)

SMC X-1: PP = 0.71 s

(Paul et al.)

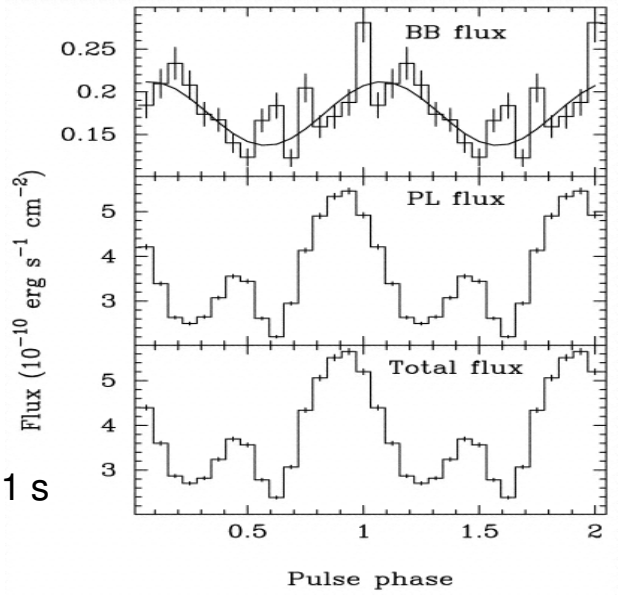

Soft Excess Emission Region

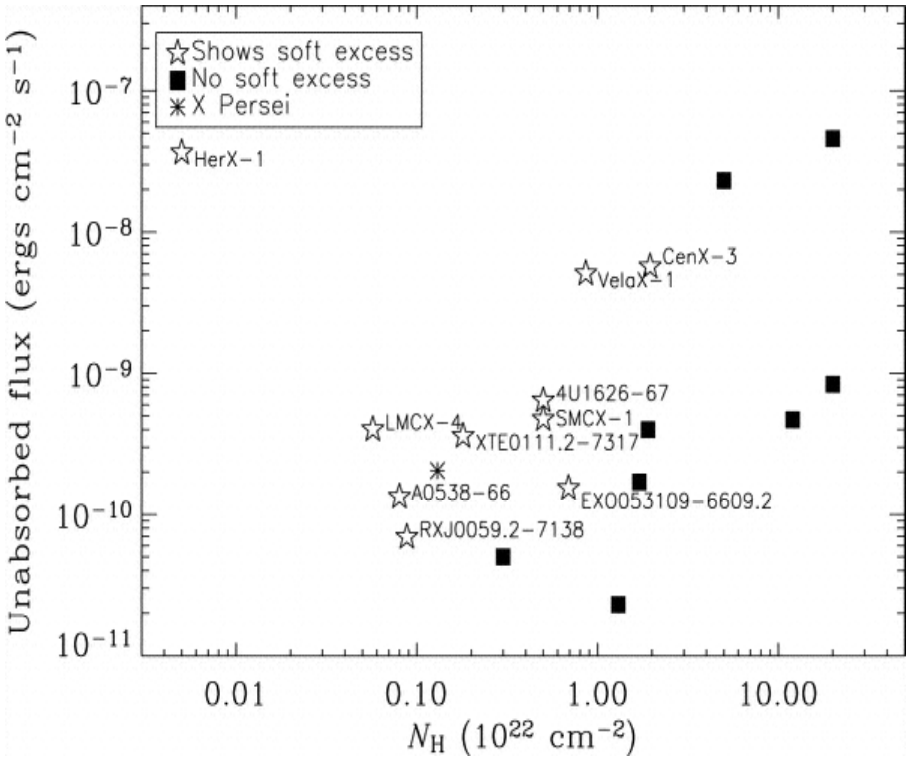

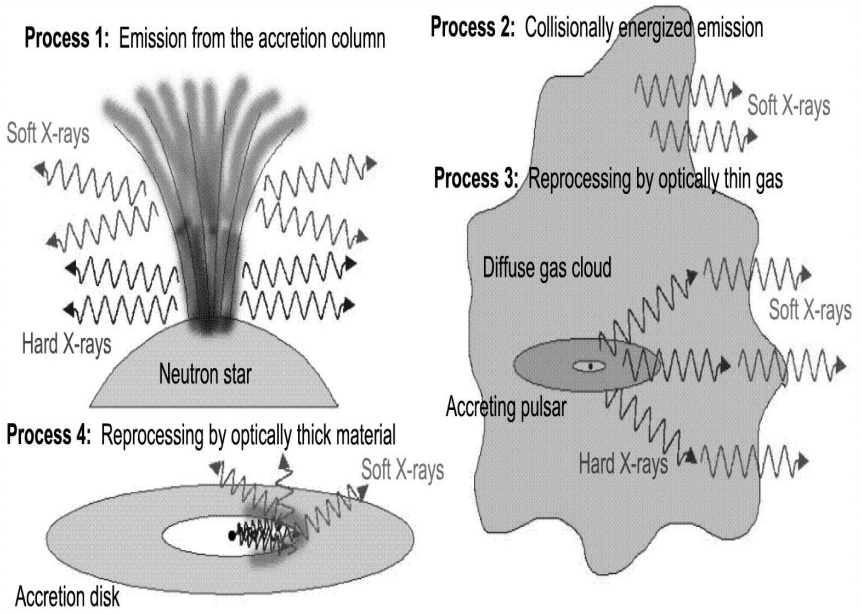

Hickox et al. 2004.

Detectable only in low absorption systems

Possible origin can be:

(a) Emission from the accretion column

(b) Collisionally energized emission

(c) Reprocessing by optically thin gas

(d) Reprocessing by optically thick material

Choice of Continuum model

Broad-band spectroscopy of GRO J1008-57 :

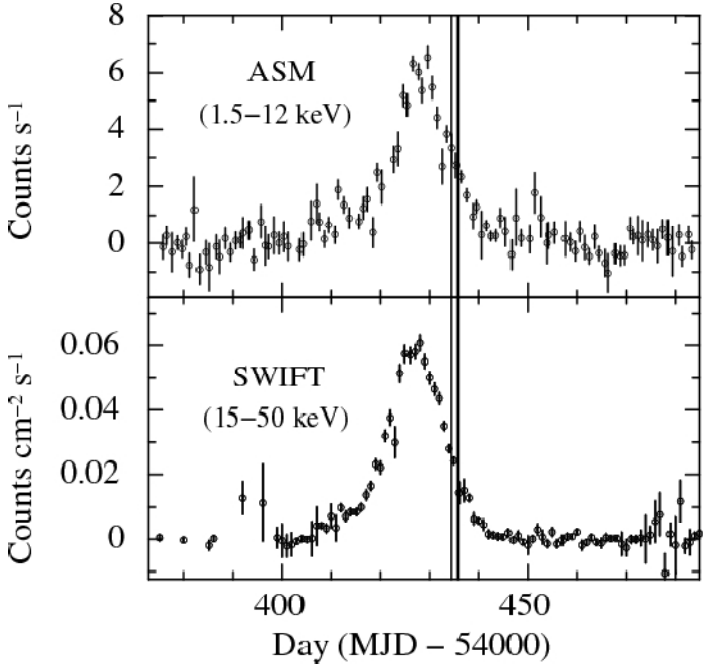

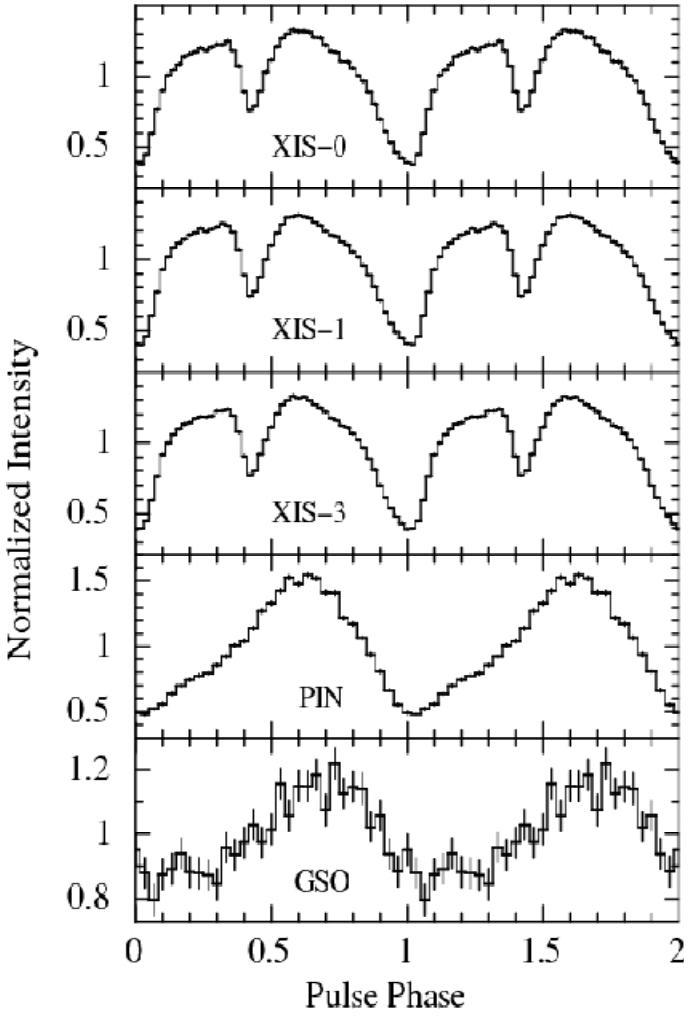

HMXB, PP~94 s

Trasient outburst was in 2007 Nov-Dec

Naik, Paul et al. (2011)

Choice of Continuum model

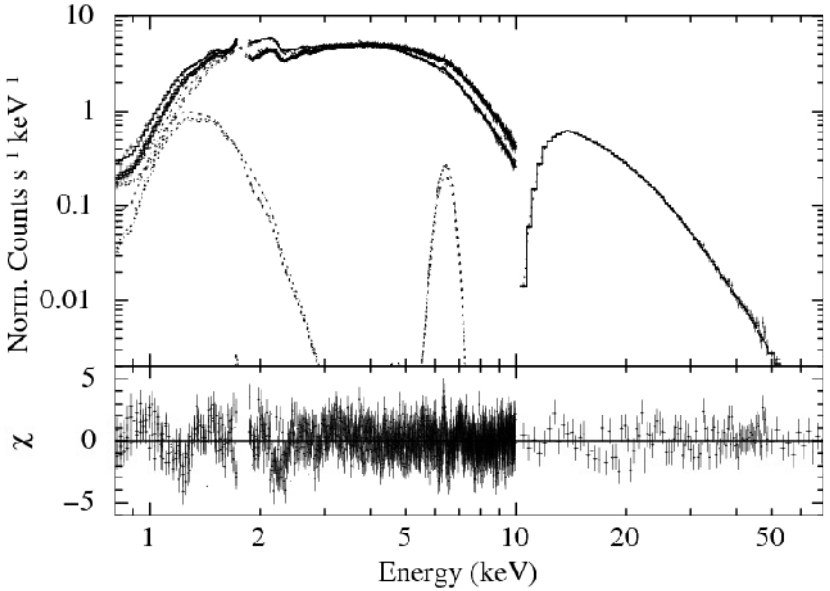

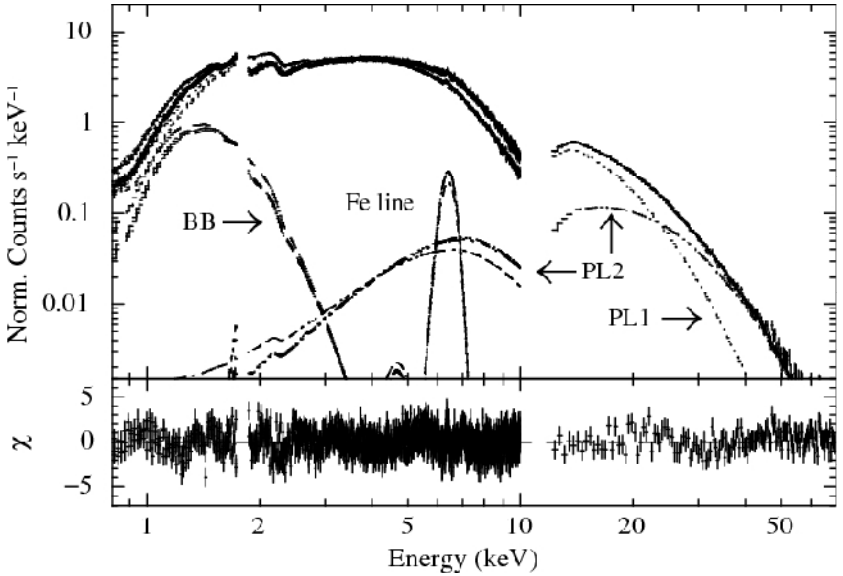

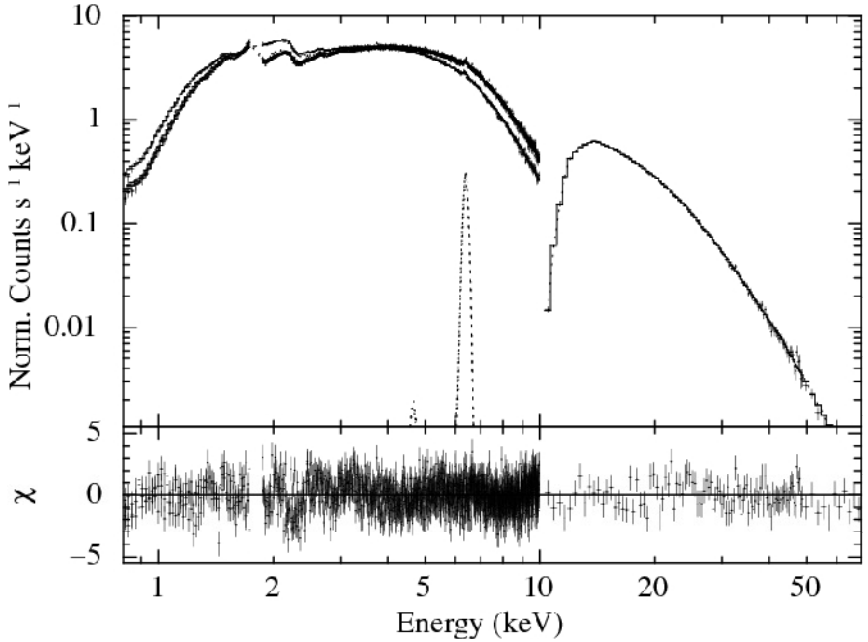

Choice of Continuum model

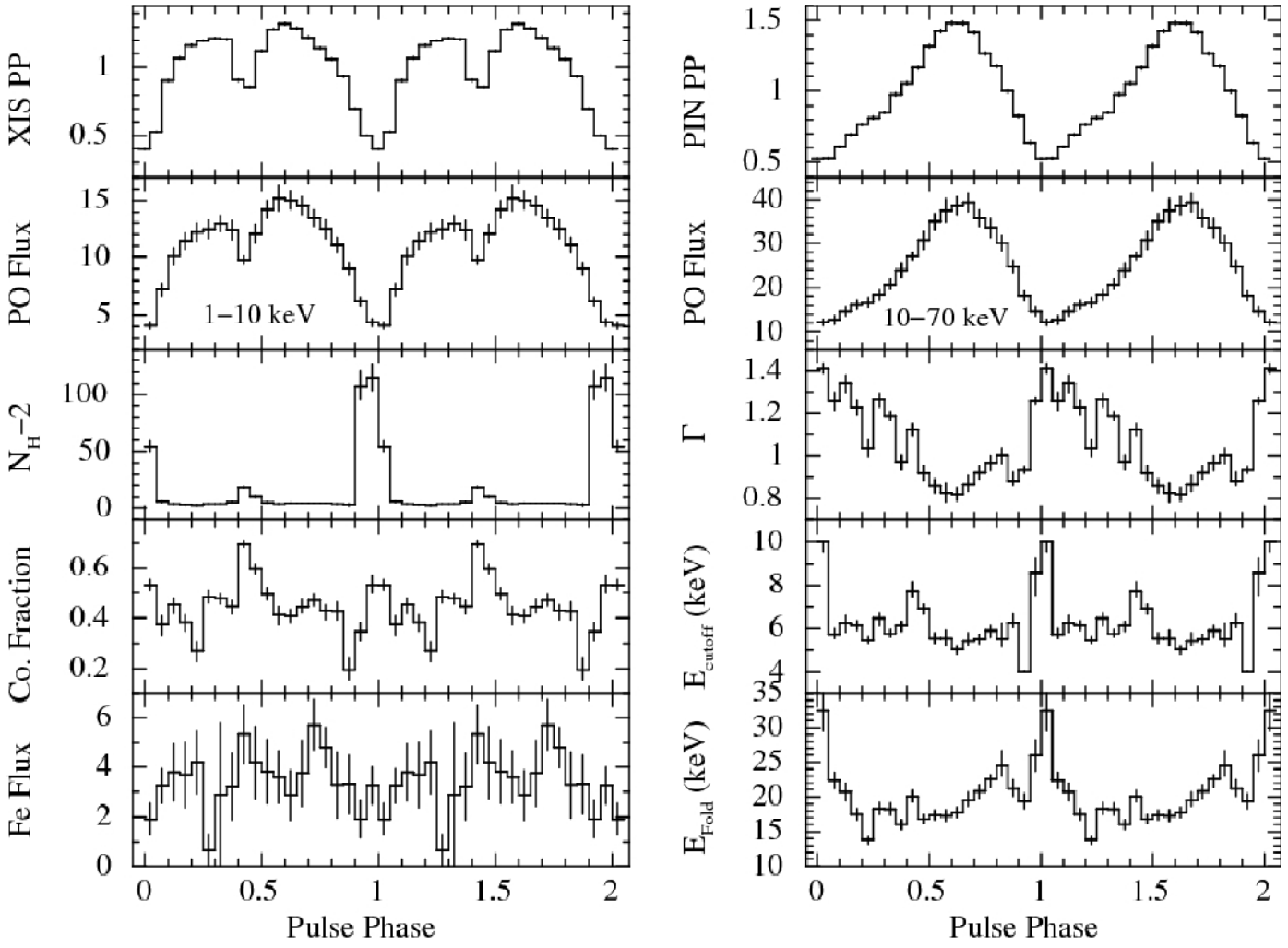

Partial covering power law model describes well to the spectra of XRB pulsars with structures in the pulse profile.

Orbital Phase Resolved Spectrum : Cen X-3

Pulse Period ~ 4.8 s, Orbital Period = 2.1 d

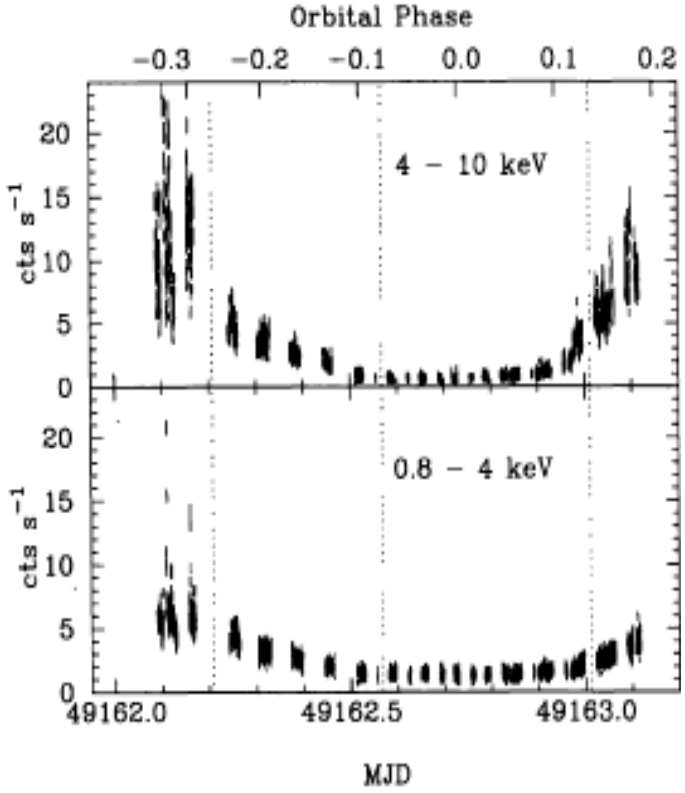

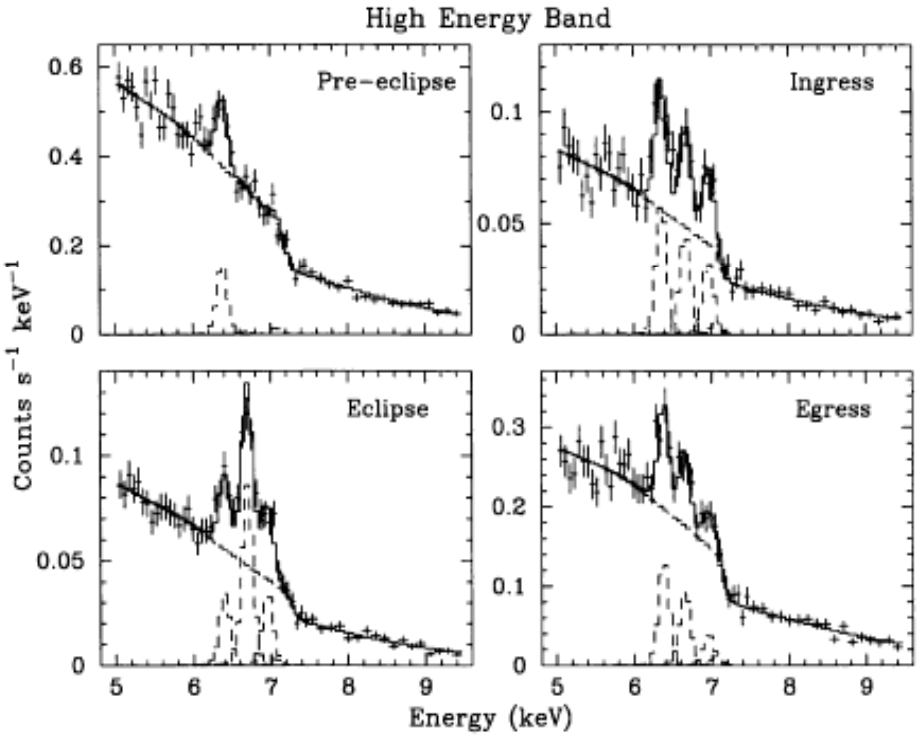

Ebisawa et al. 1996

Orbital Phase Resolved Spectrum : Cen X-3

Results from ASCA observation:

- **Clear detection of 6.4 keV, 6.7 keV, and 6.97 keV iron emission lines**
- **6.4 keV line flux decayed by an order of magnitude during the eclipse, where as the flux drop in case of other two lines were about by a factor of 3. This implies that the 6.7 keV and 6.97 keV line emission regions are much larger than the 6.4 keV line emission region.**
- **The 6.4 keV equivalent width did not show a large variation over the eclipse. Alfven shell or an optically thick accretion disk close to the neutron star are likely candidates for the origin of the fluorescent line.**

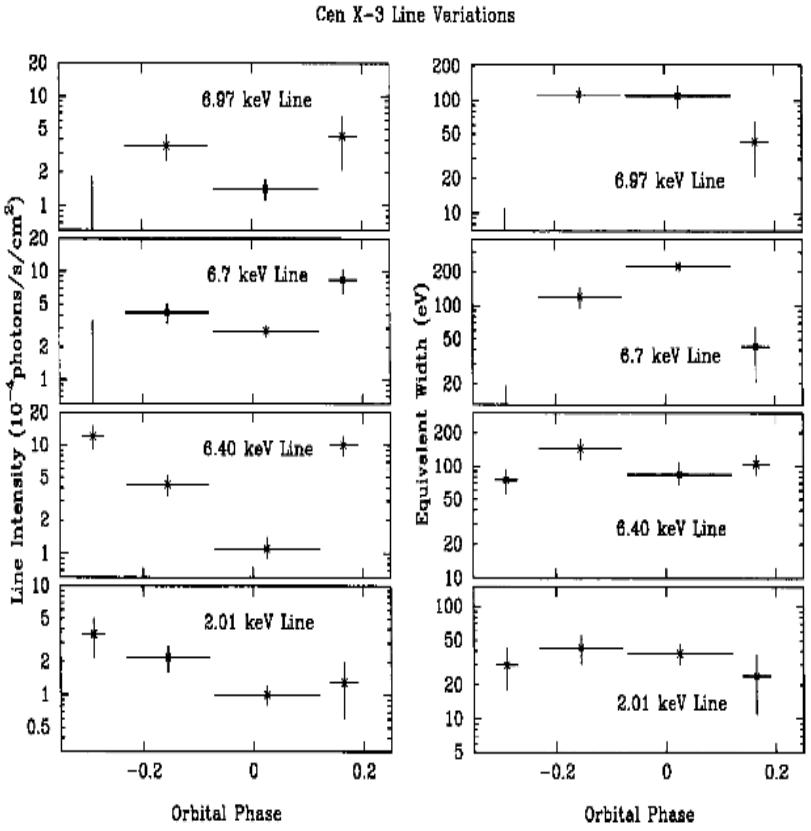

Suzaku Observation of Cen X-3

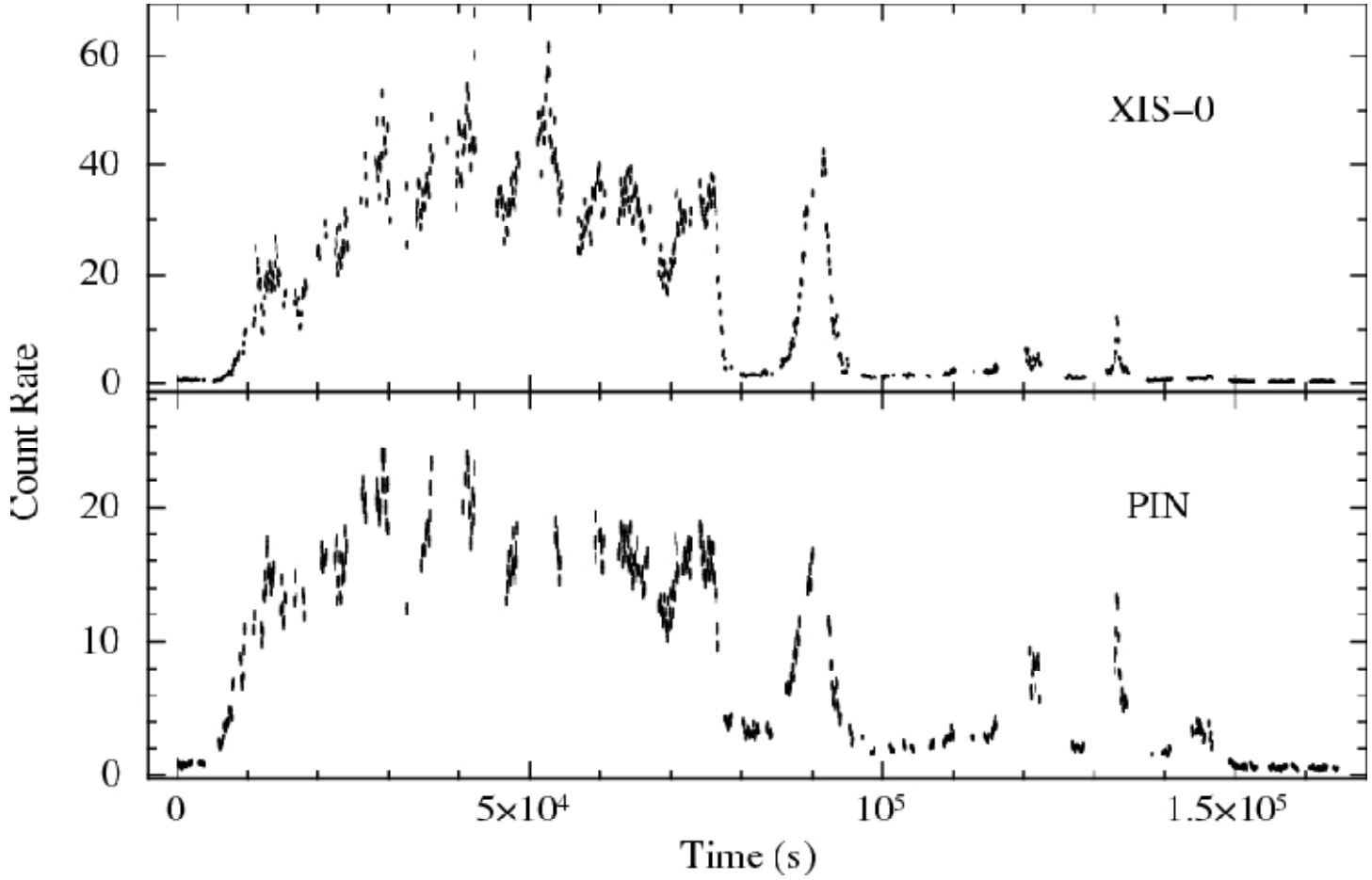

Suzaku Observation of Cen X-3

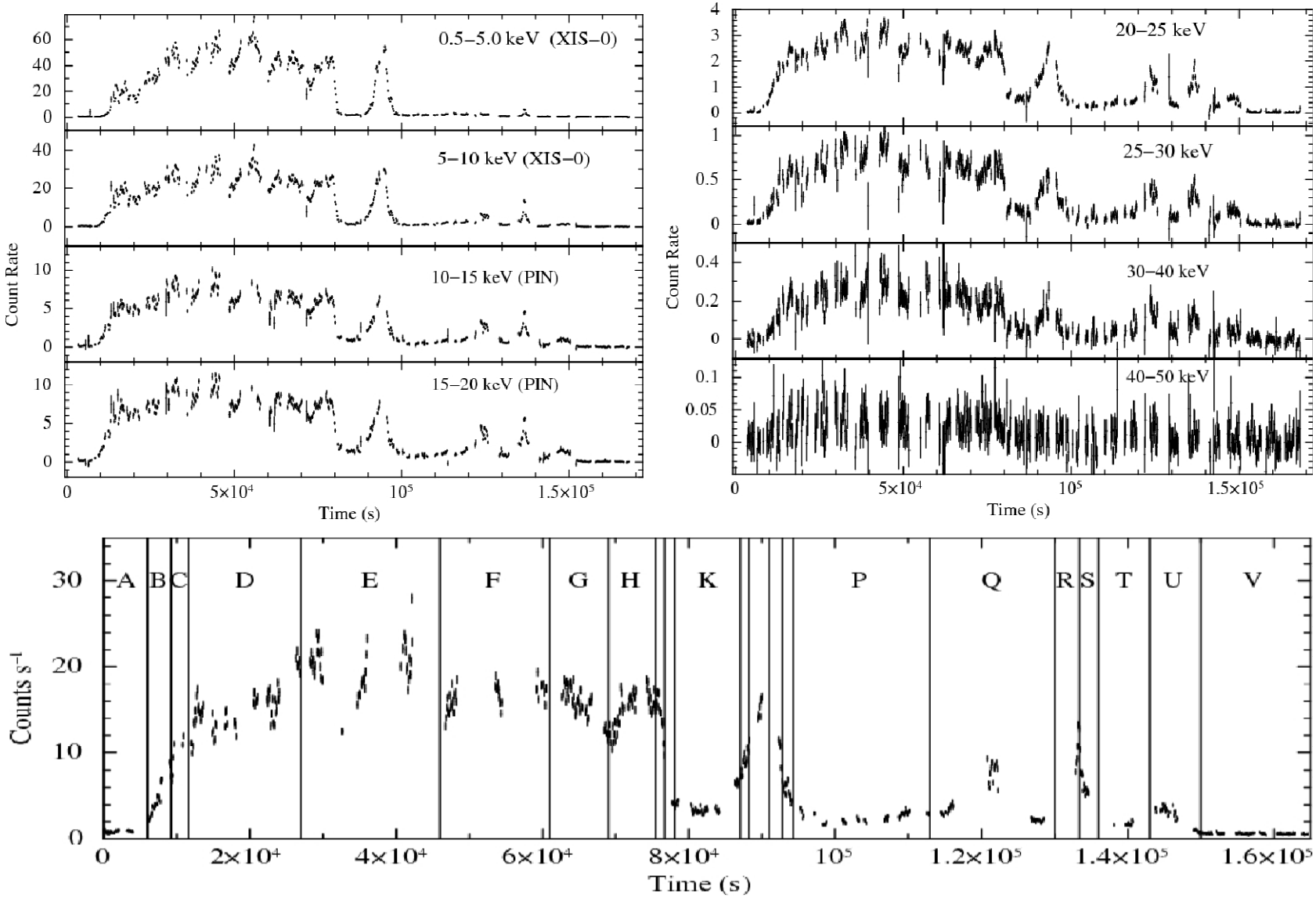

Suzaku Observation of Cen X-3

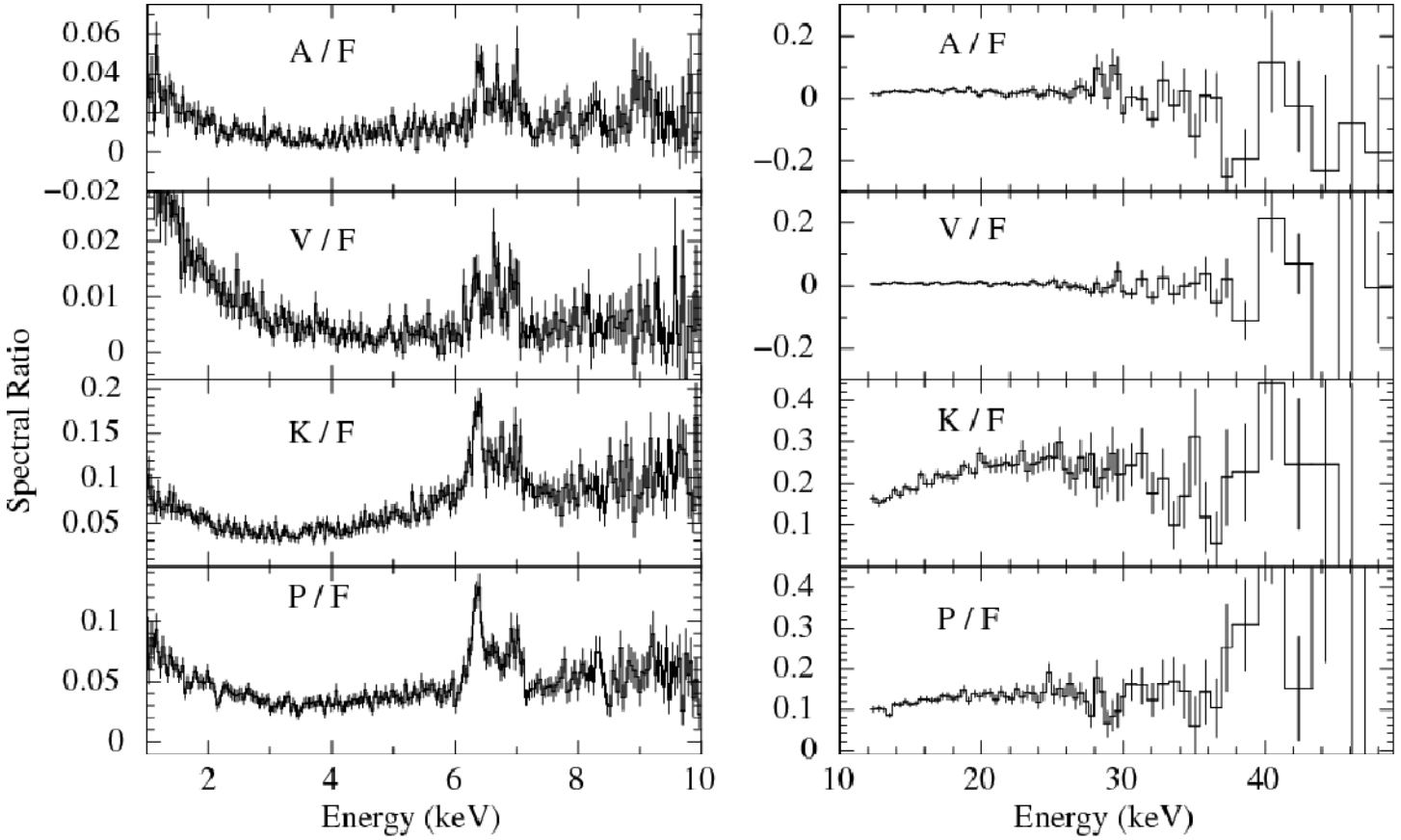

Time Resolved Spectra of Cen X-3

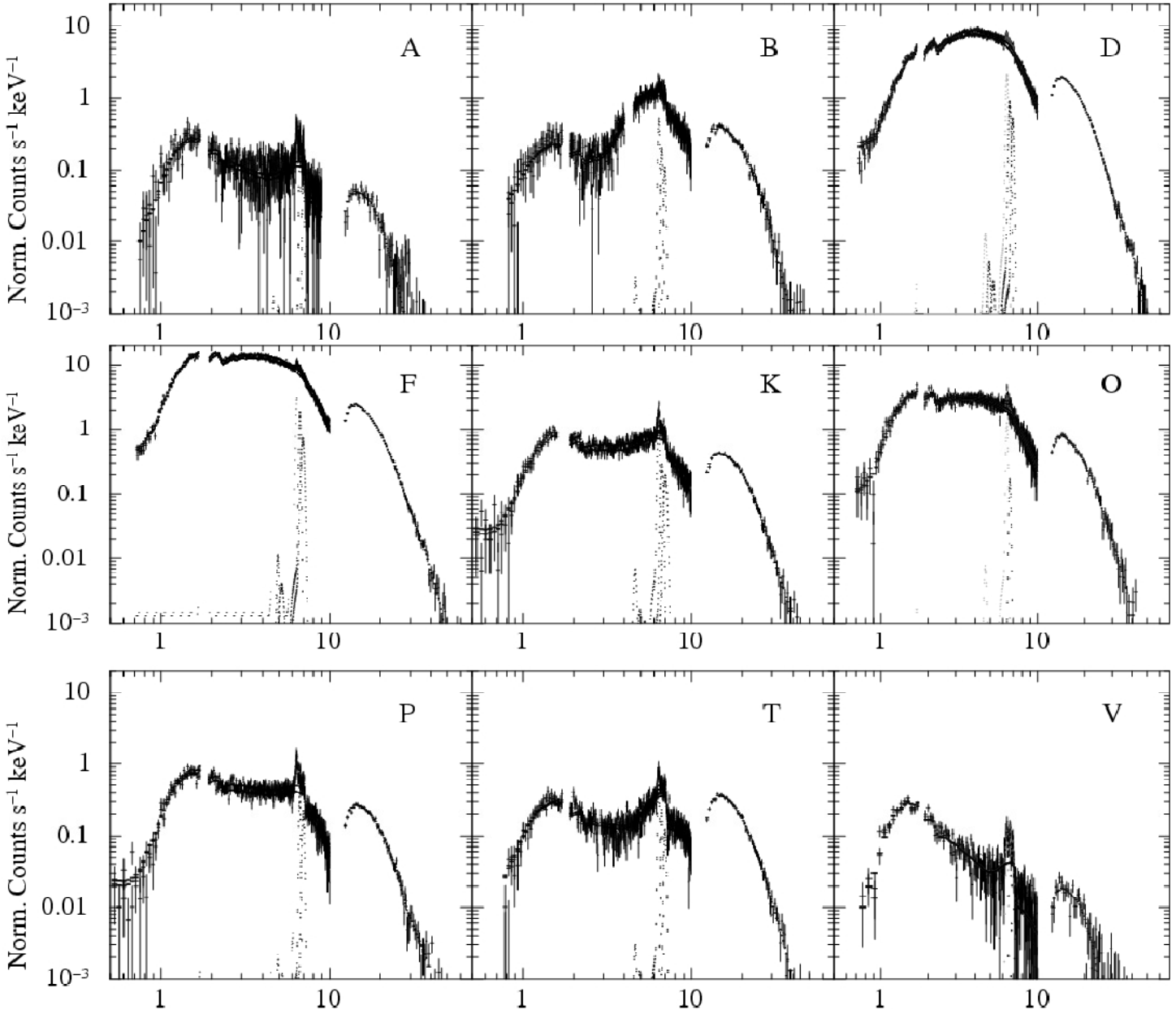

Time Resolved Spectra of Cen X-3

Spec. Reg.	N_{H1}	N_{H2}	Cov. Fraction	Photon Index	6.4 KeV line		6.7 KeV line		6.97 KeV line	
					Flux[a]	Eqw[b]	Flux[a]	Eqw[b]	Flux[a]	Eqw[b]
A	1.06±0.03	88.1±3.0	0.94±0.01	2.03±0.02	0.30±0.03	0.43±0.05	0.20±0.02	0.26±0.03	0.13±0.03	0.20±0.04
B	0.50±0.04	32.4±0.6	0.96±0.43	0.89±0.05	0.50±0.11	0.08±.02	0.24±0.11	0.03±0.02	0.16±0.09	0.03±0.01
C	2.63±0.03	3.9±0.2	0.54±0.01	0.96±0.01	1.80±0.16	0.08±0.01	0.43±0.17	0.02±0.01	$0^{+0.16}$	$0^{+0.01}$
D	1.43±0.01	2.3±0.1	0.64±0.01	0.90±0.01	2.55±0.01	0.08±0.01	1.29±0.09	0.04±0.01	0.90±0.10	0.03±0.01
E	1.01±0.01	0.9±0.1	0.57±0.01	1.03±0.01	3.55±0.10	0.07±0.01	2.69±0.10	0.06±0.01	1.46±0.14	0.03±0.01
F	1.13±0.01	1.1±0.1	0.34±0.01	1.01±0.01	3.78±0.18	0.08±0.01	1.92±0.13	0.04±0.01	1.59±0.13	0.04±0.01
G	1.13±0.01	0.9±0.1	0.29±0.01	1.01±0.01	3.32±0.12	0.09±0.01	1.85±0.13	0.05±0.01	1.41±0.16	0.04±0.01
H	1.09±0.01	1.2±0.1	0.39±0.01	0.98±0.01	3.74±0.14	0.10±0.01	1.68±0.19	0.04±0.01	0.89±0.20	0.02±0.01
I	1.30±0.01	3.8±0.3	0.34±0.01	1.08±0.01	4.12±0.30	0.10±0.01	0.87±0.29	0.02±0.01	0.88±0.30	0.02±0.01
J	1.11±0.02	3.6±0.4	0.32±0.01	0.88±0.01	2.11±0.18	0.16±0.01	0.42±0.13	0.03±0.01	1.15±0.21	0.09±0.02
K	0.95±0.02	59.8±1.0	0.86±0.01	1.20±0.01	1.23±0.05	0.28±0.01	0.43±0.06	0.09±0.01	0.44±0.06	0.10±0.01
L	1.17±0.03	9.7±0.3	0.75±0.01	0.74±0.01	3.63±0.20	0.22±0.01	1.60±0.19	0.09±0.01	1.63±0.22	0.10±0.01
M	1.04±0.01	1.9±0.2	0.28±0.01	0.84±0.01	5.19±0.30	0.17±0.01	2.62±0.29	0.08±0.01	2.92±0.32	0.09±0.01
N	1.18±0.01	2.2±0.2	0.35±0.01	1.10±0.01	2.89±0.26	0.08±0.01	1.28±0.33	0.04±0.01	0.88±0.52	0.02±0.01
O	1.29±0.02	92.9±5.4	0.47±0.01	1.01±0.01	1.30±0.15	0.11±0.01	0.21±0.11	0.02±0.01	$0.01^{+0.10}_{-0.01}$	0.01±0.01
P	0.92±0.01	79.2±1.9	0.84±0.01	1.32±0.01	0.94±0.04	0.38±0.02	0.32±0.03	0.12±0.01	0.35±0.04	0.14±0.02
Q	0.80±0.02	56.3±0.7	0.91±0.01	0.92±0.01	1.23±0.05	0.21±0.01	0.57±0.04	0.09±0.01	0.61±0.04	0.10±0.01
S	0.85±0.04	33.9±0.8	0.88±0.01	0.58±0.01	1.61±0.12	0.18±0.01	1.10±0.20	0.12±0.02	1.28±0.16	0.14±0.02
T	0.65±0.02	85.0±1.1	0.96±0.26	1.31±0.01	0.51±0.03	0.24±0.02	0.24±0.04	0.10±0.02	0.20±0.04	0.09±0.02
U	0.66±0.04	84.9±1.9	0.96±0.45	0.83±0.02	0.62±0.04	0.34±0.02	0.28±0.06	0.13±0.03	0.27±0.05	0.13±0.03
V	1.34±0.04	132.2±4.5	0.97±0.64	2.89±0.03	0.10±0.02	0.39±0.06	0.10±0.02	0.35±0.06	0.06±0.01	0.26±0.05

N_{H1} = Equivalent hydrogen column density (in 10^{22} units), N_{H2} = Additional hydrogen column density (in 10^{22} units), [a] : in 10^{-11} ergs cm^{-2} s^{-1} unit, [b] : Equivalent width (in keV).

Change in Iron Line Parameters at Different Orbital Phase

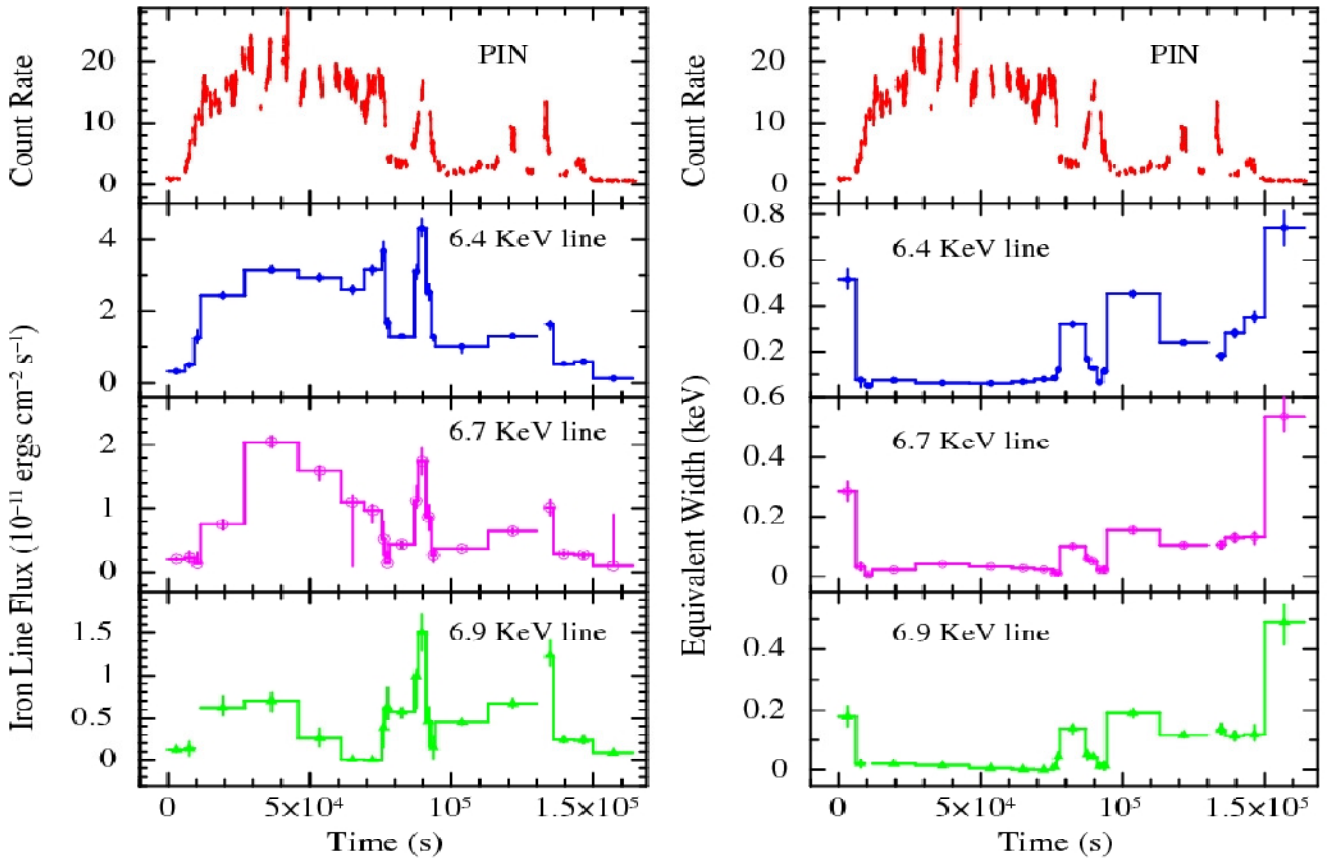

Decrease in the intensity of 6.4 keV, 6.7 keV and 6.97 keV lines during the dips

Equivalent width of the lines increases significantly during the dips

This implies the dipping feature in Cen X-3 most probably due to the presence of structures in the accretion disk as seen in LMXBs.

Cyclotron lines in Accretion-powered X-ray pulsars

Cyclotron resonance features (CRFs) are due to resonant scattering of the line of sight X-ray photons against electrons embedded in magnetic fields of the order of $10^{11}-10^{13}$ Gauss.

- **Transition between Landau levels appears in X-ray band in ~10^{12} G magnetic field pulsars**
- **A method to estimate the magnetic field of X-ray pulsars**

  [$E_a = 11.6 \times B_{12} (1+z)^{-1}$ keV]

  Magnetic fields of ~17 XRBPs have been accurately measured…
- **Luminosity dependent changes in resonance energy**

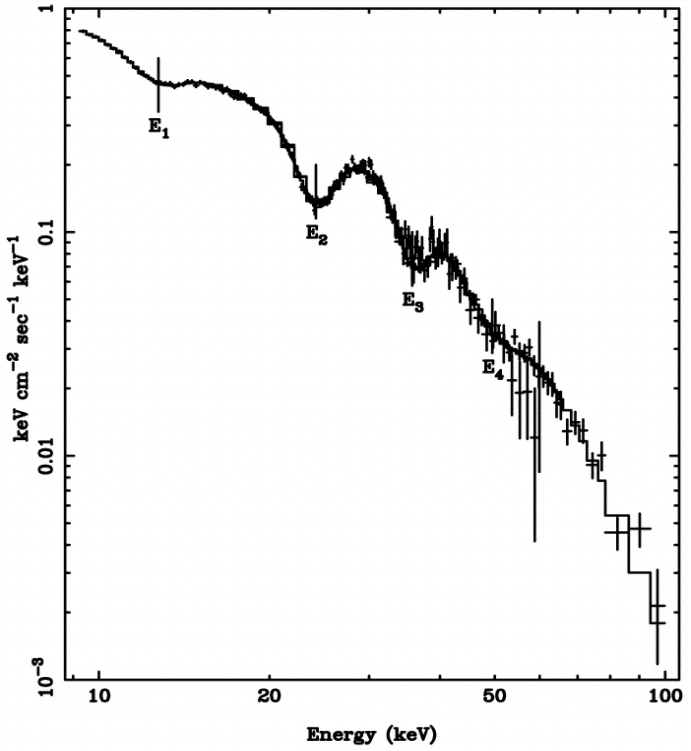

4U 0115+63: Santangelo et al. 1999

Luminosity dependent change of E_a :A0535+262

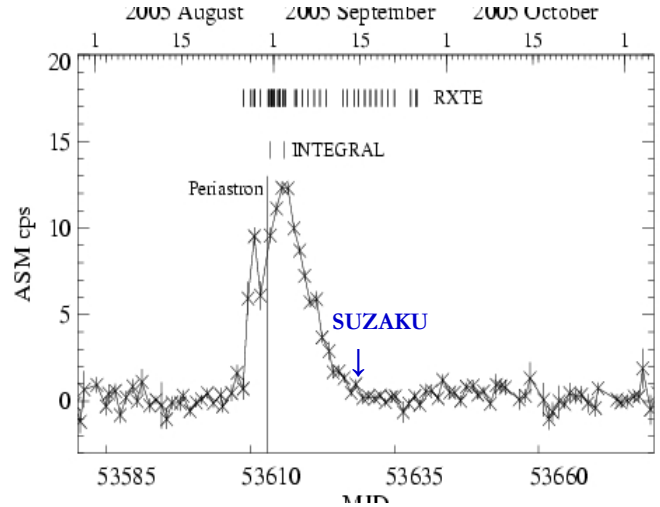

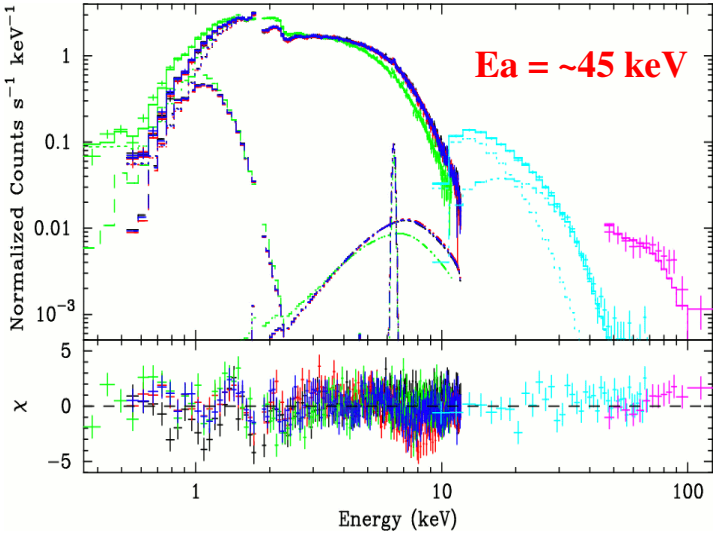

Terada et al. 2006 ; Naik et al. 2008

CRSF detected at 48.5±0.7 keV (RXTE, ATel-605), 47±2 keV (INTEGRAL, ATel-601)

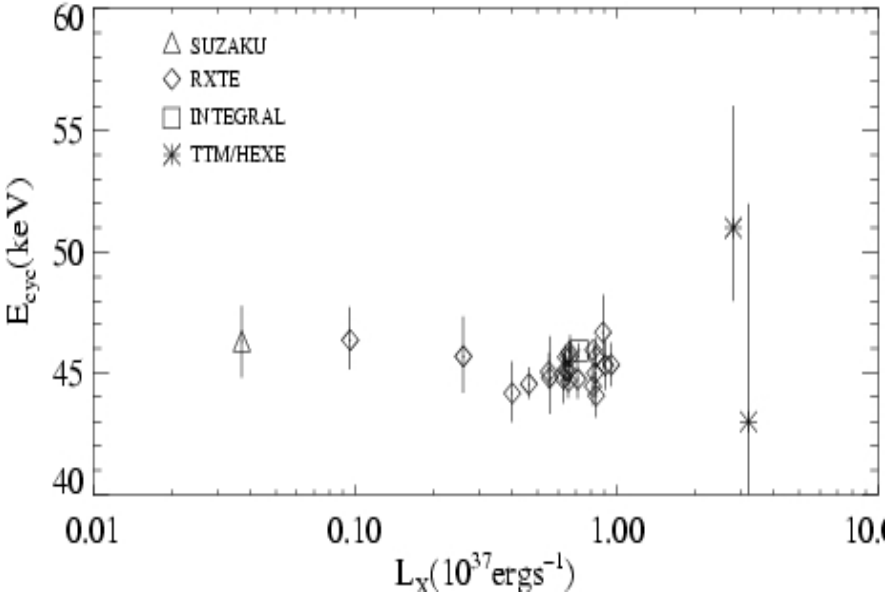

Caballero et al. 2007

B ~ 4 × 10^{12} G

Luminosity Dependent Change of E_a : (4U0115+63)

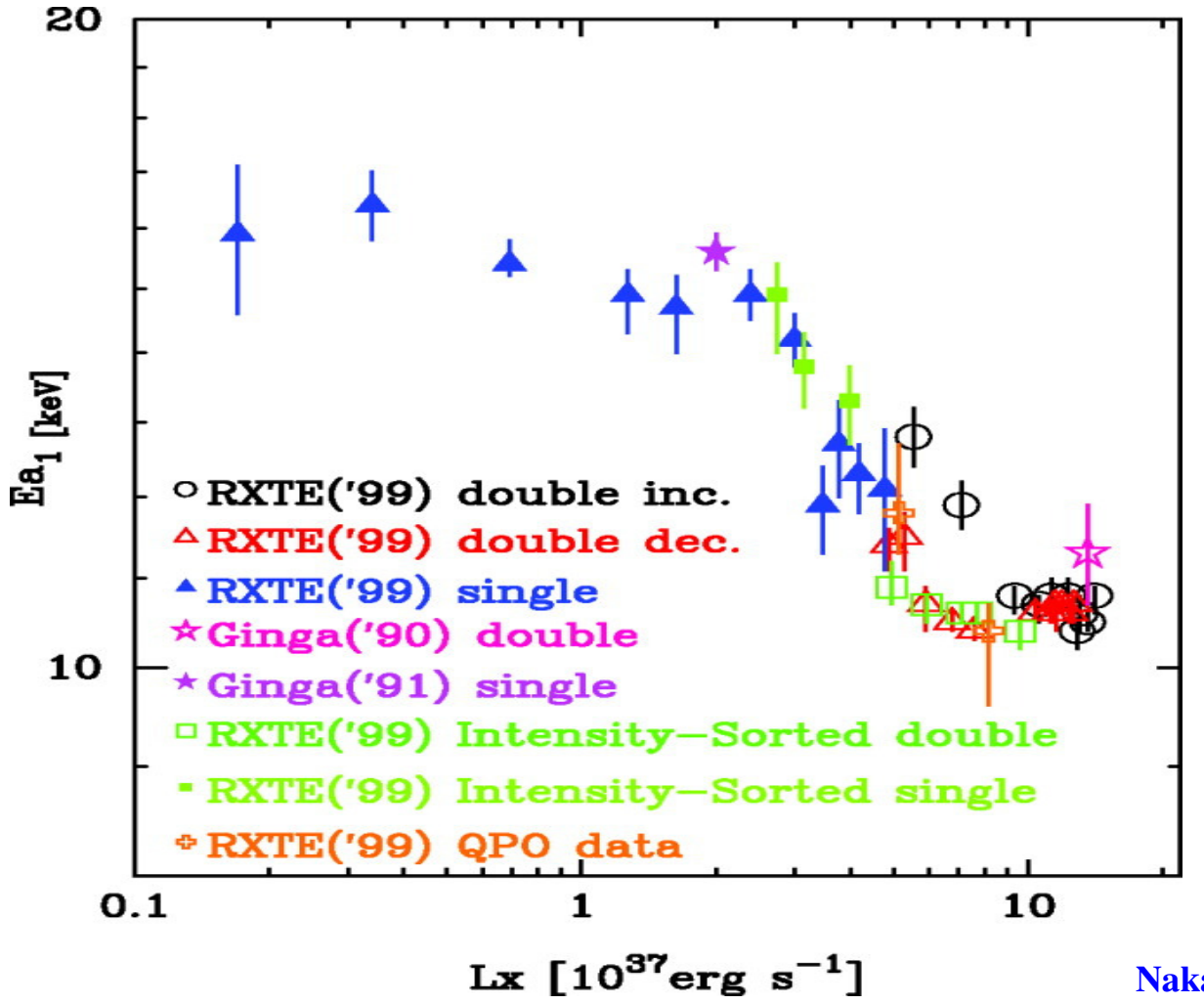

Nakajima et al. 2006

Luminosity Dependent Change of E_a

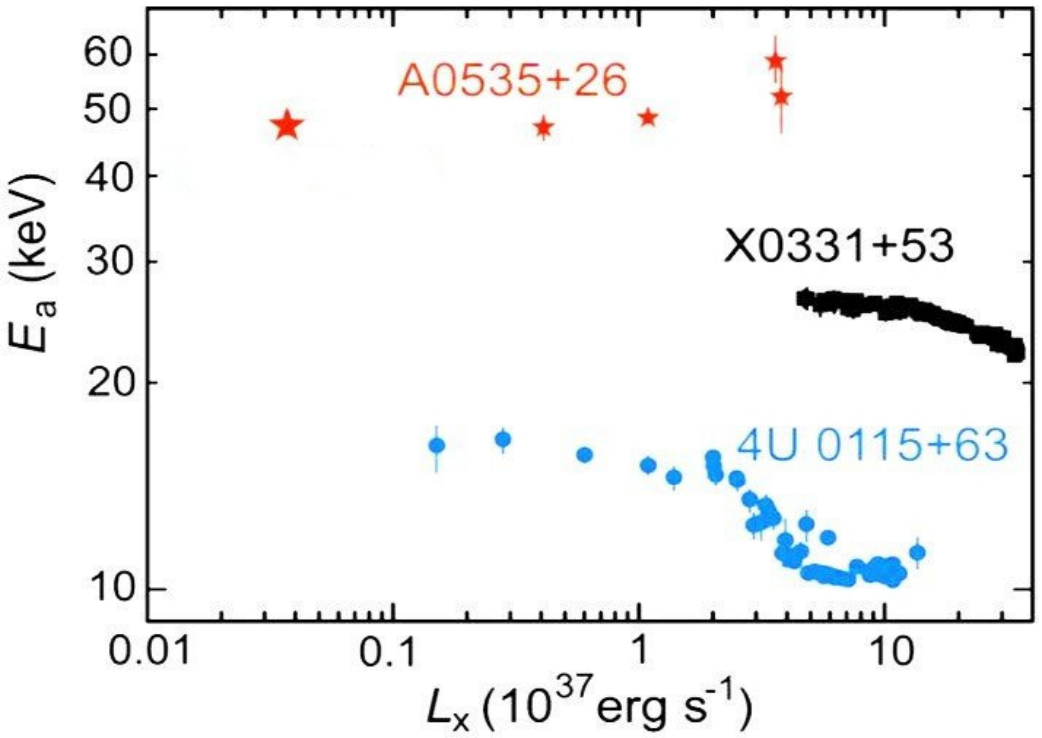

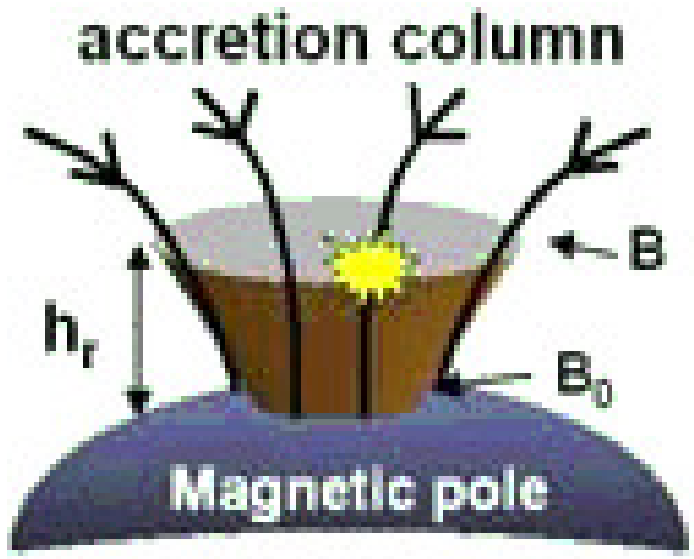

The negative luminosity dependent change can be explained by the change in the accretion column height.

$E_a \alpha (R_{NS} + h_r)^{-3}$, where h_r is the CRSF forming region. h_r can be estimated by the detection of E_a.

Summery

- *Continuum model describing the XRBP spectra*
- *Soft excess in X-ray pulsars and its origin*
- *Orbital phase resolved spectroscopy of Cen X-3*
- *Cyclotron line features in X-ray pulsars and estimation of neutron star magnetic field , luminosity dependence of the cyclotron line.*

Thanks for your attention…..